Overhauser shift of the electron spin resonance line of Si:P at the metal-insulator transition: ^{31}P contribution

U. Fasol and E. Dormann
Physikalisches Institut, Universität Karlsruhe (TH), 76128 Karlsruhe, Germany
(Received 11 December 2001; revised manuscript received 13 February 2002; published 23 August 2002)

The electron spin resonance (ESR) line of delocalized electron spins shifts upon saturation due to the hyperfine interaction with the dynamically polarized nuclear spins. The ^{31}P contribution to the ESR line's Overhauser shift is separated for phosphorus doped silicon (Si:P) in the concentration range $(2.7–7.3)\times 10^{18}/\mathrm{cm}^3$ covering the metal-insulator transition. The Overhauser shift profiles recorded versus ^{31}P nuclear magnetic resonance (NMR) frequency are nonsymmetrical and vary with P concentration. With increasing P content, their width decreases, the maximum increases, and shifts towards the bare ^{31}P nuclear Zeeman frequency. These data are compared with published results obtained by conventional ^{31}P spin-echo NMR and an early Overhauser shift measurement for Si:P. Most remarkable is the continuous variation of the frequency position of the Overhauser shift maximum across the metal-insulator transition region.

DOI: 10.1103/PhysRevB.66.075207 PACS number(s): 71.30.+h, 76.70.−r

I. INTRODUCTION

Phosphorus atoms have one electron more than Si atoms. These electrons are weakly bound in phosphorus doped silicon and their wave function is spread over several lattice constants. At P concentrations higher than a critical concentration ($N_c = 3.52\times 10^{18}/\mathrm{cm}^3$) the crystals become metallic.[1] Below this critical concentration the crystals are semiconducting and thus insulating at low temperature. The magnetic properties near the metal-insulator transition in Si:P was already a fascinating area of research for a whole generation of physicists.[2] There exists a wealth of contributions to this subject by electron spin resonance (ESR),[3–15] nuclear magnetic resonance (NMR),[2,16–27] and double-resonance techniques.[28–33] Just in the most interesting range of about 2–0.7 times N_c, information about the hyperfine interaction of the doping electron on the dopant's site is rather one sided, however.

For isolated donor electrons, the ESR line is split into two lines by the hyperfine interaction with the central ^{31}P nucleus ($I = 1/2$). At P concentration higher than about $1\times 10^{18}/\mathrm{cm}^3$, which is still lower than N_c, the exchange interaction between the nearest-neighbor electron spins is so large that most of the electron spins are no longer localized around one *P* atom. As a result, in ESR experiments only one (exchange narrowed) line is observed. Since there are not as many nuclear spins parallel as antiparallel to the external field, the electron spins still experience an average nonzero hyperfine field. But for Si:P at thermal equilibrium, at $T > 4$ K, this field is at least seven orders of magnitude smaller than the external field ($B \approx 3500$ G) for 10-GHz ESR. Since the nuclear Zeeman interaction is about a factor of 2000 smaller than that of the electron spins, it should be easier to detect the relative shift of the NMR line by the hyperfine interaction (paramagnetic shift or Knight shift). But in the vicinity of N_c the ratio of P atoms to Si atoms is only about 1:14 000. A standard NMR spectrum of ^{29}Si nuclear spins ($I = 1/2$, natural abundance 4.7%) is dominated by the Si bulk and the signal of the ^{29}Si neighbors to the P atom is wiped out. On the other hand the number of ^{31}P nuclear spins ($I = 1/2$, natural abundance 100%) in the sample is very small and the ^{31}P NMR signal is hardly detectable. In the most elaborated ^{31}P NMR analysis the observed nuclei *are associated with delocalized electrons* (*weak nonenhanced Pauli susceptibility, nuclear Korringa relaxation*).[2]

A unique possibility to learn more about the hyperfine interaction and therefore about the donor electrons close to the metal-insulator transition is to analyze the Overhauser shift of the ESR line. If the ESR transition is partly saturated, the nuclear-spin polarization is strongly increased by the so-called Overhauser effect.[34] In cw ESR experiments the frequency is kept constant, stabilized to the resonance frequency of the cavity, and the external static magnetic field is swept. The enhanced hyperfine field due to the increased nuclear-spin polarization results in a shift of the ESR line, the so-called Overhauser shift. In Si:P the resulting shift is towards the lower external field (due to a positive resulting hyperfine field[35]) and represents the integral over the effect by ^{29}Si and ^{31}P nuclear spins. In order to separate the Overhauser shift caused by the Si nuclear spins from that caused by the P nuclear spins, it is necessary to destroy the polarizations separately.[29,36] This is possible, because the NMR frequencies are different: $\nu_P/\nu_{Si} \approx 2$. Thus the hyperfine interaction at the P atom, as well as that of those Si nuclear spins which are near the P atoms, can be analyzed. Since the measurement is based on ESR, the advantage of its better signal-to-noise ratio can be utilized. The technique can be applied to conduction as well as exchange-coupled localized electrons. Thus, the local interaction at the donor site and its nearest-neighbor sites can be studied. Applications of methods based on this principle to Si:P in the semiconducting region, with $N = 0.7N_c$ and $N = 0.85N_c$, were published previously [^{29}Si,[29–31] ^{31}P (Ref. 30)]. However, no detailed study covering the metal-insulator transition has been performed up to now. Therefore, for this work, samples with $N = (2.7–7.3)\times 10^{18}/\mathrm{cm}^3$ [$N = (0.77–2.07)N_c$] have been measured at 5–11 K.[32]

We present results of a detailed ^{31}P Overhauser shift analysis of a family of Si:P samples with the phosphorus concentration range of (0.77–2.07) N_c. In the following, the samples are labeled according to their P concentration, e.g., *N*5.1.3 is sample number 3 of P concentration $5.1 \times 10^{18}/\mathrm{cm}^3$. The results of the microwave conductivity, ESR *g* factor, linewidth and saturation behavior, and the integral Overhauser shift of the ESR line, obtained with the same samples, have been published earlier as part I of the sequence.[35] A detailed analysis of simulations and measurements of the ^{29}Si contribution to the Overhauser-shift has been presented in part II.[33] Some of the results will be compared to that of the ^{31}P contribution in this paper. The structure of this paper is the following. Section II gives the experimental details. In Sec. III, the relevant theoretical relations are presented and the dependence of the change of the shift profiles on all external parameters is analyzed. A general discussion of the results and the conclusions are given in Secs. IV and V, respectively.

II. EXPERIMENTAL DETAILS

Rectangular flat samples of area ≈1.3–3.4 mm^2 and thickness 0.025–0.081 mm, i.e., less than the skin depth were prepared.[35,32] For the ESR experiments an *X*-band Bruker ESP300E spectrometer with an ER4118 dielectric resonator and an Oxford instruments cryostat was used. A probe head was developed so that, in addition to the microwave field (9.8 GHz) for the electron spins, a radiofrequency power for the ^{31}P nuclear spins (≈6 MHz) can be applied. Because the probe head with the sample and the RF coil is inserted into the high-*Q* ESR cavity, the loss of the quality factor had to be minimized. The degree of saturation of the ESR line was determined with the help of the ESR line shape.[35,32] It is given below by the saturation factor

$$s=\frac{S_0-\langle S_z\rangle}{S_0}, \tag{1}$$

where S_0 is the average value of S_z at thermal equilibrium. At full saturation the two ESR energy levels have the same occupation and so $\langle S_z\rangle=0,\ s=1$. At thermal equilibrium $\langle S_z\rangle=S_0$ and therefore $s=0$. For additional experimental details see Ref. 32.

As a first step for the measurement of the Overhauser shift profiles, the ESR line (derivative) at a constant microwave power (P_{ESR}) is recorded and the line position (B_0) is determined. The external static magnetic field (B_{Mess}) is adjusted to this field ($B_{Mess}=B_0$) and held constant (field-frequency lock). The ESR-signal amplitude at this field is then detected, while the frequency of the radio-frequency field is swept through the resonance of the ^{31}P nuclear spins. If the rf reaches the resonance frequency of some of the P nuclear spins, their polarization is reduced or destroyed, depending on the rf power. As a result the ESR line is partly shifted back (B_0 is no longer equal to B_{Mess}) and the ESR-signal amplitude at B_{Mess} changes. Using the known shape of the "virgin" ESR line obtained in the first step, it is possible to calculate from the ESR-signal amplitude at each rf the corresponding back-shift of the ESR line. Thus, the Overhauser shift profiles show at each rf frequency the contribution to the Overhauser shift caused by the ^{31}P nuclear spins resonating at this frequency. In comparison to standard ^{31}P NMR, in which the *signal amplitude* reflects only the spectrally distributed number of ^{31}P nuclear spins, for the Overhauser shift detected signal two additional pieces of information enter the *amplitude* (shift): the respective field-parallel component of the hyperfine coupling constant and the degree of Overhauser enhancement of the respective nuclear-spin polarization. All shift values reported below for ^{31}P are positive. This means that the ESR line shifts to higher external field, if the corresponding ^{31}P contribution is eliminated by NMR saturation. Thus, the dynamically polarized ^{31}P nuclear spins must have a positive hyperfine field contribution to the ESR field.

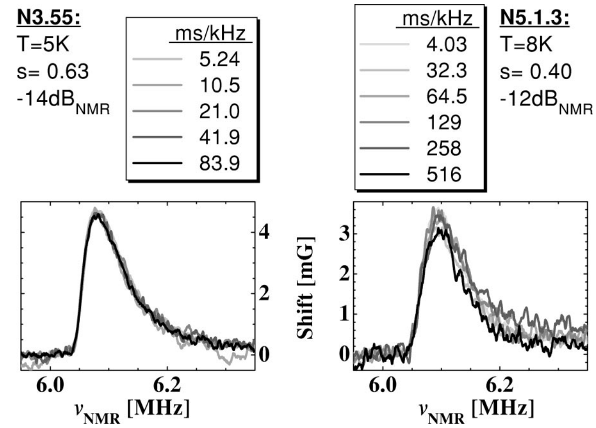

FIG. 1. The Overhauser shift profiles of sample *N*3.55 at 5 K and *N*5.1.3 at 8 K measured with different rf sweep velocities.

III. ANALYSIS OF THE EXPERIMENTAL RESULTS

A. A typical measured ^{31}P Overhauser shift profile

The typical form of ^{31}P Overhauser shift profiles can be seen, e.g., in Fig. 1. Its asymmetric form is caused by the distribution of hyperfine interactions within the ^{31}P system. The Overhauser shift profiles caused by the ^{29}Si nuclear spins also show an asymmetric form of considerably smaller width.[33] By comparison to simulations it could be shown that the distribution within the ^{29}Si nuclear-spin system primarily reflects the distribution of Si-P atomic distances. For the ^{31}P nuclear spins there is one electron spin per P atom, but the P atoms are distributed randomly in the crystal.[37] Hence there are regions with higher and others with lower P densities. Thus the asymmetry of the ^{31}P Overhauser shift profiles means that the resulting hyperfine fields must be different in regions with different local P densities. The spectra of a few classical NMR measurements reported in the literature are also asymmetric up to the highest analyzed P-concentration ($N=1.4\times10^{20}/\mathrm{cm}^3$).[2,16–18,20] We refer here to Ref. 2 for a detailed discussion of the relevant mechanisms for this asymmetry.

In principle, it is possible to build up an Overhauser enhanced nuclear-spin polarization via both the anisotropic dipolar and the isotropic Fermi contact hyperfine interaction.[38]

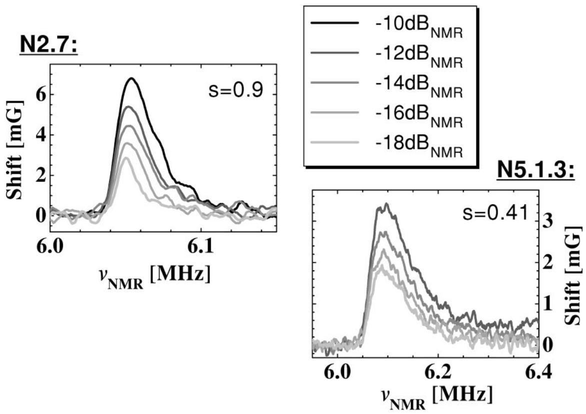

FIG. 2. Change of the measured shift profile at $T=5.3$ K with increasing rf power (0 dB_{NMR} corresponds to approximately 30 W).

The resulting polarization and therefore the Overhauser shift have opposite signs depending on the relative magnitudes of these two interactions. The sign of the shift in the profile of the P nuclear spins of this study shows—not unexpectedly—that the Fermi contact interaction is the dominant interaction for the ^{31}P nuclear spins in Si:P. The same is also true for the ^{29}Si nuclear spins.[33]

B. The dependence on rf sweep time and on rf power

Decreasing spin lattice relaxation times[16] and time constants of building up the nuclear-spin polarization by the Overhauser effect[30] with increasing nuclear-spin resonance frequency within the ^{31}P spectrum are reported in the literature. This can be explained by the distribution of hyperfine interaction strengths. But experiments with different rf sweep velocities showed (see Fig. 1) that the ^{31}P nuclear spins are polarized quickly enough and the form of the profiles analyzed in this work is not spoiled by time-dependent processes [which was observed for ^{29}Si (Ref. 33).] The same method as used for ^{29}Si in our earlier report[33] was used to confine the time constants of the dynamic ^{31}P nuclear-spin polarization. It turns out that the time constants must be shorter than 1 ms, which is our current instrumental limit. Hence these time constants are clearly shorter than the spin lattice relaxation times reported by Alloul and Dellouve[16] (2–16 ms), which is in accordance with the advantage of the Overhauser shift technique to monitor preferentially the strongly hyperfine interacting nuclear spins.

The degree of nuclear-spin polarization, which is destroyed by the radio-frequency power (P_{NMR}) for the nuclear spins, depends on P_{NMR}. Thus at constant microwave power (P_{ESR}) and the therefore constant ESR line saturation, the magnitude of the Overhauser shift profile increases with increasing P_{NMR} (see Fig. 2). The increase of the extremum has a saturationlike behavior

$$Shift_{max}=O_{\mathrm{shi}}\frac{\beta P_{NMR}}{1+\beta P_{NMR}} \tag{2}$$

because the polarization of the nuclear spins can at best be reduced to zero. In addition, a shift of the peak position can be observed with increasing P_{NMR} in Fig. 2. This reveals that it is comparatively easier to saturate the NMR transitions exhibiting small hyperfine fields.

C. Influence of the degree of ESR saturation

The ESR saturation has two different effects on the electron and the nuclear-spin system. As mentioned before there is a distribution of hyperfine interaction strengths within the P nuclear-spin system. For each distinct group of ^{31}P nuclear spins i, characterized by the strength and type of hyperfine interaction, the hyperfine field monitored by the electron spins and therefore the contribution to the Overhauser shift is given by

$$\Delta B_i=\frac{8\pi}{3}\hbar\gamma_P I_0(1-sV_P^i)|\psi_i(0)|^2\frac{n_i}{n_{tot}}, \tag{3}$$

where γ_P is the gyromagnetic ratio of the P nuclear spins; $\langle I_z\rangle=I_0(1-sV_P^i)$: I_0 is the average nuclear-spin polarization $\langle I_z\rangle$ in thermal equilibrium, s is the ESR-saturation factor, and V_P^i is the enhancement factor for the ^{31}P nuclear-spin polarization caused by the Overhauser effect;[38] $|\psi_i(0)|^2$ is the electron Fermi contact density at the P nuclei of group i; (n_i/n_{tot}) is the share of the P nuclear spins of group i in comparison to all P nuclear spins in the sample. The nuclear-spin polarization is enhanced by the Overhauser effect. Therefore the Overhauser shift increases with increasing ESR saturation and with it the amplitude of the Overhauser shift profiles. The enhancement factor V_P^i is proportional to the ratio γ_e/γ_P (γ_e is the gyromagnetic ratio of the electron spins). The maximum possible enhancement for the ^{31}P nuclear spins in Si:P is -1622, but it can be reduced by leakage processes.[38] If the isotropic hyperfine interaction predominates, the leakage is negligible. But if additional relaxation paths for the nuclear spins exist, the enhancement of the nuclear-spin polarization is reduced.

On the other hand, the ESR saturation affects via the hyperfine interaction also the resonance of the nuclear spins. Since they are subjected to an additional field, caused by the electron spins, their resonance frequency is shifted by

$$\Delta\nu_i=\nu_0\left(\frac{8\pi}{3}\frac{\hbar\gamma_e}{B_{Mess}}S_0^i(1-s)|\psi_i(0)|^2\right) \tag{4}$$

$$=\nu_0\left(\frac{8\pi}{3}\chi_e^i(1-s)|\psi_i(0)|^2\right), \tag{5}$$

where ν_0 is the nuclear-spin resonance frequency caused by the bare nuclear Zeeman interaction, $\langle S_z\rangle^i=S_0^i(1-s)$ is the average local electron-spin polarization, and $\chi_e^i(1-s)$ is the local susceptibility. At this location, also the electron-spin characteristics are important. They change from more Curie-like localized but exchange-coupled moments to Pauli-like delocalized spins. With increasing ESR saturation the electron-spin polarization is reduced and as a result the shift of the nuclear-spin resonance frequency decreases. At total saturation of the electron spins ($s=1$) $\Delta\nu_i=0$ and the posi-

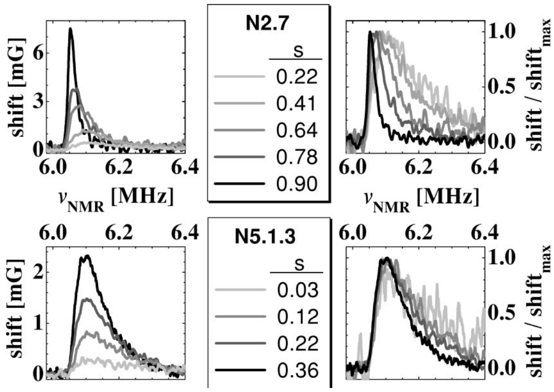

FIG. 3. The measured profiles of samples $N2.7$ and $N5.1.3$ at 5.3 K for different degrees of ESR saturation. The figures on the right side show the same profiles normalized to the maximum.

tion of the Overhauser shift profile on the NMR frequency scale is shifted to the resonance frequency by the bare nuclear Zeeman interaction.

The results of the measurements for samples $N2.7$ and $N5.1.3$ at 5.3 K are shown in Fig. 3. The increase of the shift height with increasing degree of saturation can be clearly observed on the left side. On the right side the corresponding diagrams are shown with normalized height. In these diagrams, the reduction of the width and the shift to a smaller frequency with increasing ESR saturation can be observed. The effect is more clearly visible for sample $N2.7$, because a higher degree of ESR saturation could be reached in this case.

D. Influence of the temperature

Each shift value of the Overhauser shift profile versus NMR frequency is proportional to the thermal average nuclear-spin polarization I_0 [Eq. (3)] and therefore proportional to $1/T$ (Curie law). The profiles of sample $N2.7$ (see Fig. 4) seem to follow the Curie law within the accuracy of the measurement. On the other hand, the heights of the profiles of the samples with higher P concentration do not increase, as would be expected by the Curie law. Extrapolating the shift maximum at each ESR saturation factor to P_{NMR}

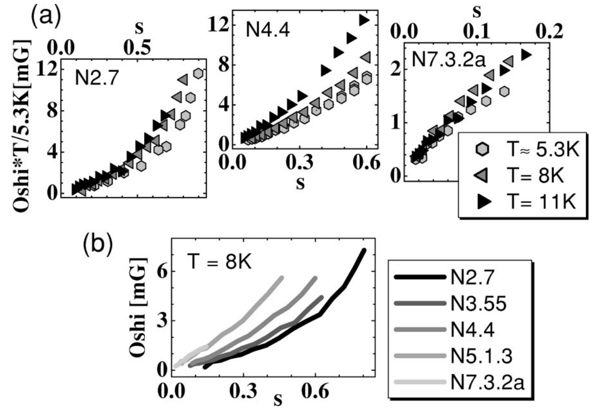

FIG. 5. Height of the extremum of the Overhauser shift profiles, extrapolated to rf power $\rightarrow\infty$ ($O_{\rm shi}$) versus the ESR saturation factor. (a) For $N2.7$, $N4.4$, and $N7.3.2a$ for different temperatures. To eliminate the influence of the Curie law on the average nuclear-spin polarzation, the values have been converted to about 5.3 K. (b) At 8 K for varied P concentration. (The curve for sample $N7.3.2a$ is very similar to that of sample $N5.1.3$ at small ESR-saturation factor.)

$\rightarrow\infty$, a shift-related quantity ($O_{\rm shi}$) is derived, which is independent of P_{NMR} [Eq. (2)]. The extrapolated shift peak heights multiplied with the temperature of the measurement and divided by the minimum temperature $T_{min}\approx 5.3$ K should be independent of T for each sample, if the Curie law is the only temperature-dependent process. The results of $N2.7$ and $N7.3.2a$ seem to show a domination of the Curie law at least for a small ESR-saturation factor [see Fig. 5(a)]. But in the curves of $N3.55$, $N4.4$, and $N5.1.3$ additional temperature-dependent processes are observed [see, e.g., for $N4.4$ in Fig. 5(a)].

E. Influence of the P concentration

The shape of the P Overhauser shift profiles becomes increasingly narrow with increasing P concentration (Fig. 6, large diagram). In addition, the peak moves to smaller frequencies. This means that the homogeneity of the samples increases with increasing P concentration and that P nuclear spins in regions with high P densities experience a smaller

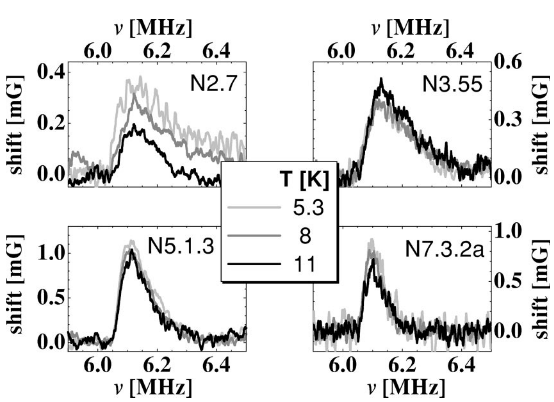

FIG. 4. Overhauser shift profiles of sample $N2.7$ ($s\approx 0.17$), $N3.55$ ($s\approx 0.18$), $N5.1.3$ ($s\approx 0.18$), and $N7.3.2a$ ($s\approx 0.14$) at 5.3, 8, and 11 K (-13 dB$_{NMR}$).

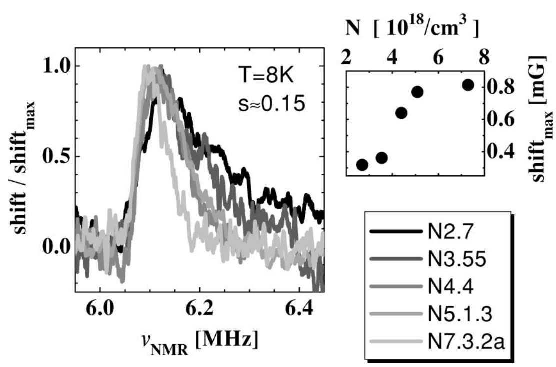

FIG. 6. ^{31}P Overhauser shift profiles, measured with different P concentration at 8 K (-13 dB$_{NMR}$). The profiles are normalized to the maxima. The heights are shown in the small figure above the legend.

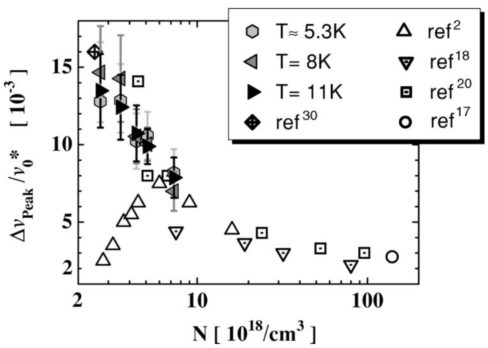

FIG. 7. Relative shift of the position of the ^{31}P Overhauser shift profile peak versus P concentration in Si:P. The critical concentration for the metal-insulator transition is $N_c = 3.52\times10^{18}/cm^3$. For comparison the results of ^{31}P NMR spin-echo experiments [Ref. 2, $T=4.2$ K; $\nu_0^* = {}^{31}P$ NMR line of H_3PO_4; Ref. 18, $T=4.2$ K ($N = 7.5\times10^{18}/cm^3$, $T=1.85$ K); $\nu_0^* = {}^{31}P$ NMR line of GaP; Ref. 20, $T=0.6$ K; $\nu_0^* = {}^{31}P$ NMR line of GaP; Ref. 17, $T=4.2$ K, $\nu_0^* = {}^{31}P$ NMR line of GaP] and one Overhauser shift measurement, Ref. 30: $T=1.3$ K (ν_0^* , not mentioned), given in the literature are also shown.

hyperfine field than P nuclear spins in regions with low P density. The amplitude of the maximum increases with increasing P concentration (Fig. 6, small diagram). The extrapolated maximal heights at 8 K versus the ESR-saturation factor [Fig. 5(b)] show that the slope of the curves increases with increasing P concentration.

Figure 7 shows the relative shift of the ^{31}P Overhauser shift profile peak versus P concentration. The error bars include the standard deviation [profiles at several P_{NMR} and small P_{ESR} ($s \ll 1$) have been analyzed] and the deviation caused by the fact that $s>0$. The error introduced by using the start of the flank as reference ν_0^* was determined by extrapolation of the peak position to $s=1$. It is smaller than the accuracy of the determination of $\Delta\nu_{peak}/\nu_0^*$.

IV. DISCUSSION

An important question for the interpretation of the Overhauser shift measurement is of course, whether all ^{31}P nuclear spins in the respective Si:P sample are monitored. The electrons of interest originate from the dopant P atoms. However, the presence of conduction electrons or a minimum of exchange interaction between the ''localized'' electron spins are required for the measurement. Then there is only one motionally or exchange narrowed ESR line, and the kinetic energy or the exchange interaction serve as an energy reservoir for building up an enhanced nuclear-spin polarization.[38] Isolated P atoms are not integrated in the Overhauser shift measurement. The analysis of the ESR lines with increasing ESR saturation[35] indicates that in the samples $N2.7$ and $N3.55$ there are still different regions, where the electron spins do not communicate between these regions. But even at sample $N2.7$ no ESR signal could be found, within the accuracy of the measurement, at positions where ESR lines split by hyperfine interaction should be found. Hence the number of isolated P atoms must be very small in the observed samples, and the measurements presented in this paper include the majority of the ^{31}P nuclear spins, however with a varying enhancement factor [see Eq. (3)].

With increasing ESR-saturation factor the ESR line is shifted by a superposition of the ^{31}P and ^{29}Si contribution (integral shift[35]) to a lower magnetic field. Since the isotropic hyperfine interaction (Fermi contact interaction) dominates for the ^{31}P and ^{29}Si nuclei and the shifts caused by ^{31}P and ^{29}Si have opposite sign, the observed integral shift proves that the influence of the ^{31}P nuclear spins is larger than that of the ^{29}Si nuclear spins. Since the electron wave function has its center at the P atom, it is expected that the electron density is much larger at the P nuclei than at the Si nuclear spins in the neighborhood. But the observed magnitude of the ^{29}Si Overhauser shift profiles are much larger (up to 130 mG) than that of the ^{31}P nuclear spins. For calculating the integral shift it is necessary to sum up the contributions of all distinct subgroups of ^{29}Si and ^{31}P nuclear spins. Then the small amplitude of the ^{31}P Overhauser shift profiles is overcome by the large width, which is at half maximum, a factor $\approx 22-50$ larger than that of the ^{29}Si Overhauser shift profiles.

The integral shift[35] and the extrapolated extremal heights of the ^{29}Si profiles[33] show a similar and simple temperature-dependent behavior. It is dominated by the Curie law of the average nuclear-spin polarization. Only small deviations can be observed for $N \geq 4.4\times10^{18}/cm^3$. This has been explained by temperature-dependent leakage processes, which seem to gain more influence with increasing P concentration above N_c. In contrast, especially the results of the ^{31}P Overhauser shift measurement of the samples $N3.55$, $N4.4$, and $N5.1.3$ do not really support a proportionality to $1/T$. Since the integral shift of the ESR line is nevertheless dominated by the Curie law,[35] the deviation of the ^{31}P profiles is likely to be caused by the distribution of local suceptibility and electron-spin characteristics and the distribution of leakage processes.

A comparison of the Overhauser shift profiles of the ^{31}P contribution with that of the ^{29}Si nuclear spins[33] shows the whole NMR frequency spread of the ^{31}P nuclear spins is larger by a factor of $\approx 8-27$ than that of the ^{29}Si distribution. A factor of 2 can be explained by the relation of the gyromagnetic ratios of the ^{31}P and ^{29}Si nuclear spins. Since the electron contact density at Si nuclear spins near the P atoms is at least a factor of 10 smaller than that at the P nucleus itself,[28] the reduced width of the ^{29}Si profile can be explained. Measurements of the susceptibility have shown a decreasing total electronic susceptibility with increasing P concentration in the analyzed range.[2,5,7,39–41] This seems to have no striking influence on the ^{29}Si Overhauser shift profiles dominated by the distribution of Si-P distances.[33] In addition, it was observed that the hydrogenlike form of the wave function does not change within the accuracy of the measurement in the range of P concentrations under consideration [$N = (2.7-7.3)\times10^{18}/cm^3$].[33] This fits to the result of Ref. 2 that the contact density at the ^{31}P nucleus does not vary substantially in the narrow concentration range studied there. Since the distribution of the hyperfine interaction within the ^{31}P nuclear spins is caused by the random distribution of the P atoms in the sample and therefore by the inhomogeneity of the electron system, the change of the susceptibility has a significant effect on the ^{31}P Overhauser shift profiles. Because of the decreasing total susceptibility with increasing P concentration it is expected that in regions with high P atomic density the local electronic susceptibility is smaller than in regions with low P density in the sample. This is confirmed by the narrowing of the ^{31}P Overhauser shift profiles and the shift of the profile peak to smaller ^{31}P NMR frequencies for increasing P-concentration of the sample, which is found in an increasing probability of regions with relatively high P density. There is a clear difference to the behavior of the ^{31}P NMR spectra in the same concentration range,[2] because these reflect only the behavior of ^{31}P nuclei, which sense conduction-band electron states with a *T*-independent susceptibility. Only the decrease of the width and the peak shift of the ^{31}P NMR in the metallic range for $N \geqslant 6\times10^{18}/\mathrm{cm}^3$ parallels the ^{31}P Overhauser shift results. Nevertheless the observed increase of the normalized ^{31}P NMR linewidth ($\Delta H/\langle K\rangle H_0$; $\langle K\rangle$, average Knight shift) with decreasing N was interpreted as an indication of an increasing distribution of χ_e for the observed sites.[2] On the other hand, the results of the Overhauser shift analysis follow more closely the total electronic magnetic susceptibility that was plotted in Fig. 9 of Ref. 2 than the NMR data. The results of the peak shift obtained with the Overhauser shift profiles show a continous variation from nonmetallic to metallic samples and connect smoothly the pioneering Overhauser shift data for $N=2.5\times10^{18}/\mathrm{cm}^3$ (Ref. 30) and the NMR data in the metallic region with higher P concentration[2,17,18,20] (see Fig. 7). Within the accuracy of the measurement no jump at N_c is observable.

V. CONCLUSION

Measurements of the ESR-line Overhauser shift profiles caused by the ^{31}P nuclear-spin polarization in Si:P in the concentration range $(0.77–2.07)N_c$ close to the metal-insulator transition are reported. The relevant theoretical relations for the Overhauser shift profiles are presented and the dependence of the shift profiles on experimental parameters such as rf sweep time, rf power, and ESR saturation are analyzed. On the basis of these insights the change of the profiles with P concentration and temperature are analyzed and interpreted.

The time constants for building up the ^{31}P dynamic spin polarization are less than 1 ms. The shape of the ^{31}P Overhauser shift profile is highly asymmetric like the spectrum of standard ^{31}P NMR,[2,16] because it is dominated by the distribution of hyperfine interaction strength reflecting the random distribution of P atoms and therefore the inhomogeneity of the electron system. The change of local susceptibility depending on the phosphorus concentration has a predominating influence on the form of the profiles. The narrowing of the profiles and the shift of its peak show that the local electron susceptibility decreases with increasing local P density. This is in accordance with the change of the total electron magnetic susceptibility plotted in Fig. 9 of Ref. 2. This experimental information merits a detailed theoretical consideration.

The relative peak shift observed by the ^{31}P Overhauser shift results and the ^{31}P NMR results for $N\geqslant6\times10^{18}/\mathrm{cm}^3$ shows a continuous variation from nonmetallic samples with $N=2.5\times10^{18}/\mathrm{cm}^3$ to metallic samples with $N=1.4\times10^{20}/\mathrm{cm}^3$ with an asymptotic behavior with increasing P concentration. Whereas the results and conclusions from the ^{31}P NMR and ^{31}P Overhauser shift analyses of Si:P in the metallic range for $N\geqslant6\times10^{18}/\mathrm{cm}^3$ are equivalent, the information content of both techniques is complementary for lower P concentration. The Overhauser shift is confirmed to be the appropriate method to survey the local hyperfine interaction near the metal-insulator transition, because the exchange-coupled localized as well as the metallic delocalized electrons contribute to the results.

ACKNOWLEDGMENTS

We thank H. v. Löhneysen for providing the samples and E. Borie for a critical reading of the manuscript. This work was financially supported by the Deutsche Forschungsgemeinschaft within the Sonderforschungsbereich 195 (Universität Karlsruhe).

[1] H. Stupp, M. Hornung, M. Lakner, O. Madel and H.v. Löhneysen, Phys. Rev. Lett. **71**, 2634 (1993).
[2] H. Alloul and P. Dellouve, J. Phys. Colloq. **49**, C8-1185 (1988).
[3] J.H. Pifer, Phys. Rev. B **12**, 4391 (1975).
[4] Sh. Maekawa and N. Kinoshita, J. Phys. Soc. Jpn. **19**, 2240 (1964); **20**, 1447 (1965).
[5] H. Ue and Sh. Maekawa, Phys. Rev. B **3**, 4232 (1971).
[6] J.D. Quirt and J.R. Marko, Phys. Rev. B **5**, 1716 (1972).
[7] J.D. Quirt and J.R. Marko, Phys. Rev. B **7**, 3842 (1973).
[8] Y. Ochiai and E. Matsuura, Phys. Status Solidi A **38**, 243 (1976).
[9] P. Swarup and P.L. Trivedi, Fiz. Tverd. Tela **18**, 323 (1976) [Sov. Phys. Solid State **18**, 190 (1976)].
[10] Y. Toyada, N. Kishimoto, K. Murakami, and K. Morigaki, J. Phys. Soc. Jpn. **43**, 114 (1977); Y. Toyoda and K. Morigaki, *ibid.* **43**, 118 (1977).
[11] E.M. Gershenzon, I.T. Semenov, and M. S. Fogel'son, Sov. Phys. Semicond. **18**, 263 (1984) [Fiz. Tekh. Poluprovodn. **18**, 421 (1984)].
[12] M.A. Paalanen, S. Sachdev, R.N. Bhatt, and A. E. Ruckenstein, Phys. Rev. Lett. **54**, 1295 (1986).
[13] A. Stesmans, Phys. Status Solidi B **143**, 733 (1987).
[14] V. Zarifis and T.G. Castner, Phys. Rev. B **36**, R6198 (1987).
[15] P.J. Mason and D.P. Tunstall, J. Phys.: Condens. Matter **3**, 8095 (1991).
[16] H. Alloul and P. Dellouve, Phys. Rev. Lett. **59**, 578 (1987).
[17] R.K. Sundfors and D.F. Holcomb, Phys. Rev. **136**, A810 (1964).
[18] G.C. Brown and D.F. Holcomb, Phys. Rev. B **10**, 3394 (1974).

[19] W. Sasaki, S. Ikehata, and Sh. Kobayashi, J. Phys. Soc. Jpn. **36**, 1377 (1974).
[20] S. Ikehata, W. Sasaki, and Sh. Kobayashi, J. Phys. Soc. Jpn. **39**, 1492 (1975).
[21] Sh. Kobayashi, Y. Fukagawa, S. Ikehata, and W. Sasaki, J. Phys. Soc. Jpn. **45**, 1276 (1978).
[22] M.A. Paalanen, A.E. Ruckenstein, and G.A. Thomas, Phys. Rev. Lett. **54**, 1295 (1985).
[23] J.R. Meyer and F.J. Bartoli, Philos. Mag. B **52**, L51 (1985).
[24] M.J. Hirsch and D.F. Holcomb, Phys. Rev. B **33**, 2520 (1986).
[25] M.J.R. Hoch and D.F. Holcomb, Phys. Rev. B **38**, 10 550 (1988).
[26] M.J.R. Hoch, U. Thomanschefsky, and D.F. Holcomb, Physica B **165&166**, 305 (1990).
[27] S.T. Stoddart, M.J.R. Hoch, and U. Thomanschefsky, Phys. Rev. B **46**, 10 007 (1992).
[28] G. Feher, Phys. Rev. **114**, 1219 (1959).
[29] D. Jerome, Ch. Ryter, and J.M. Winter, Physics (Long Island City, N.Y.) **2**, 81 (1965).
[30] D. Jerome, Ch. Ryter, H.J. Schulz, and J. Friedel, Philos. Mag. B **52**, 403 (1985).
[31] V. Dyakonov and G. Denninger, Phys. Rev. B **46**, R5008 (1992).
[32] U. Fasol, Ph.D. thesis, Universität Karlsruhe, 2001; U. Fasol, *Messung der Overhauserverschiebung an Si:P im Bereich des Metall-Isolator-Übergangs* (Shaker Verlag, Aachen, 2001).
[33] U. Fasol and E. Dormann, Eur. Phys. J. B (to be published).
[34] A.W. Overhauser, Phys. Rev. **92**, 411 (1953).
[35] U. Fasol and E. Dormann, J. Phys.: Condens. Matter **13**, 10065 (2001).
[36] G. Denninger, *Advances in Solid State Physics* (Vieweg, Braunschweig, 1990), Vol. 30, p. 113.
[37] T. Trappmann, Ch. Sürgers, and H.v. Löhneysen, Europhys. Lett. **38**, 177 (1997).
[38] A. Abragam, *The Principles of Nuclear Magnetism* (Oxford University Press, London, 1961).
[39] A. Roy, M. Turner, and M.P. Sarachik, Phys. Rev. B **37**, 5522 (1988); A. Roy and M.P. Sarachik, *ibid.* **37**, 5531 (1988).
[40] H.G. Schlager, Ph.D. thesis, Universität Karlsruhe, 1996; H.G. Schlager, *Zur magnetischen Suszeptibilität von phosphordotiertem Silizium am Metall-Isolator-Übergang* (Shaker Verlag, Aachen, 1997).
[41] Y. Ootuka and N. Matsunaga, J. Phys. Soc. Jpn. **59**, 1801 (1990).